Pergamon

Geochimica et Cosmochimica Acta, Vol. 67, No. 16, pp. 3033–3044, 2003

0016-7037/03 $30.00 + .00

doi:10.1016/S0016-7037(00)00197-2

Experimental determination of the activity of chromite in multicomponent spinels

RONIT KESSEL,* JOHN R. BECKETT, and EDWARD M. STOLPER

Division of Geological and Planetary Sciences, MC 170-25, California Institute of Technology, Pasadena, CA 91125, USA

(*Received November* 26, 2001; *accepted in revised form June* 24, 2002)

Abstract—We determined activity–composition relationships in Pt-Cr and Pt-Fe-Cr alloys at 1300°C experimentally and used the results to constrain the thermodynamic properties of chromite–picrochromite spinels. The Pt-Cr binary is characterized by strong negative deviations from ideality throughout the investigated composition range and the activity–composition relationship can be fit by a four-suffix asymmetric regular solution with three binary interaction parameters. The ternary alloy was modeled as a four-suffix asymmetric regular solution; the three ternary interaction parameters in this model were constrained by combining interaction parameters for the three bounding binaries taken from this and previous work with results for a set of experiments in which the activity of Cr in Pt-Fe-Cr-alloys was fixed by coexisting Cr_2O_3 at known f_{O_2}.

The free energy of formation of $FeCr_2O_4$ at 1300°C was determined using the activities of Fe and Cr in Pt-alloys in equilibrium with oxide mixes of $FeCr_2O_4$ and Cr_2O_3. The free energy of formation of chromite from $Fe+Cr_2O_3+O_2$ is -202.7 ± 0.4 kJ/mol (1σ), indistinguishable from literature values. The corresponding free energy of formation of $FeCr_2O_4$ from the elements is -923.5 ± 2.1 kJ/mol (1σ), and the enthalpy of formation at 298 K is -1438 kJ/mol. The activity–composition relationship for the chromite component in $(Fe,Mg)Cr_2O_4$ solid solutions was determined from a set of experiments in which Pt-alloys were equilibrated with spinel + Cr_2O_3. $(Fe,Mg)Cr_2O_4$ spinels are nearly ideal at 1300°C; modeling our data with a one-site symmetric regular solution yields an interaction parameter of $+2.14 \pm 0.62$ kJ/mol (1σ), similar to values based on data from the literature.

1. INTRODUCTION

Although spinel is usually an accessory mineral, it occurs in a wide variety of igneous and metamorphic rocks on the Earth and other planets, making it a valuable indicator of petrologic processes. For example, changes in the Cr or Ti contents of spinels are linked to the degree of partial melting in planetary mantles and to crystallization/differentiation of basaltic magmas (El Goresy, 1976; Dick and Bullen, 1984; Arai, 1987), to variations in metamorphic grade in terrestrial serpentinites (e.g., Evans and Frost, 1975), and to both igneous crystallization and subsolidus reduction processes in meteorites (Haggerty, 1972). Spinel is also commonly used in constructing geothermometers, geobarometers, and oxygen barometers. For example, the coexistence of a magnetite–ulvöspinel solid solution with a hematite–ilmenite solid solution, a common occurrence in terrestrial igneous rocks (e.g., Carmichael, 1967), allows temperature and oxygen fugacity to be constrained simultaneously (Buddington and Lindsley, 1964).

The wide range of rock types in which spinel occurs makes it versatile for constraining the origin and evolution of rocks but calculation of precise and accurate pressures, temperatures, and/or oxygen fugacities is possible only if the activity–composition relationships are well constrained. This is problematic for spinels, even though they are structurally simple, because natural spinels are compositionally complex (e.g., there are often significant concentrations of six or more different cations substituting into the two crystallographically distinct sites), ordering of cations between sites can be a strong function of composition and temperature (e.g., Sack and Ghiorso, 1991a,b), and Fe and sometimes other cations occur in multiple valence states.

Although petrologic applications of spinel thermochemistry almost always involve compositionally complex spinels, experimental studies designed to obtain thermodynamic properties have generally been limited to binary and rarely ternary subsystems, and most involve magnetite as an end member [e.g., Fe_3O_4-$MgFe_2O_4$, Fe_3O_4-$FeAl_2O_4$, Fe_3O_4-$MgAl_2O_4$ (Mason and Bowen, 1981; Nell et al., 1989; Nell and Wood, 1989); Fe_3O_4-Fe_2TiO_4 (Katsura et al., 1975; Woodland and Wood, 1994); Fe_3O_4-$FeCr_2O_4$ (Katsura et al., 1975; Petric and Jacob, 1982); $FeAl_2O_4$-$FeCr_2O_4$ (Petric and Jacob, 1982); $FeCr_2O_4$-$MgCr_2O_4$ (Hino et al., 1994; Jacob and Iyengar, 1999), $MgAl_2O_4$-Fe_3O_4-$\gamma Fe_{3/8}O_4$ (Mattioli et al., 1987)]. Results from these simple subsystems form the basis of activity–composition models for multicomponent natural spinels (e.g., Sack, 1982; Sack and Ghiorso, 1991a,b).

Chromium is an essential constituent of many spinels in terrestrial crustal and mantle rocks and in meteorites, so the activity–composition relationships for Cr-bearing spinels are key to full utilization of spinel-bearing assemblages for thermometry and barometry. One way to determine the activity of the chromite component, $FeCr_2O_4$, in multicomponent spinels is to equilibrate them with a Pt-alloy at known temperature and oxygen fugacity and then measure the Fe and Cr contents of the alloy. If the activity coefficients of Fe and Cr in the alloy are known, the activity of the chromite component can then be readily calculated. In this paper, we determine the activity–composition relationships of ternary Pt-Fe-Cr alloys (a key ingredient for measuring the thermodynamic properties of multicomponent Cr-, Fe-bearing spinels based on equilibrium with Pt-alloys) by equilibrating them with Cr_2O_3 and simple Cr-, Fe-bearing spinels at known temperature and oxygen fugacity.

* Author to whom correspondence should be addressed, at Institute of Mineralogy and Petrography, ETH-Zentrum, CH-8092 Zürich, Switzerland (kessel@erdw.ethz.ch).

We also show how such experiments can be used to determine the free energy of formation of end-member $FeCr_2O_4$ and activity–composition relationships for binary chromite–picrochromite ($MgCr_2O_4$) spinels at 1300°C. This is necessary preparatory work for applying our technique to determine experimentally chromite activities in spinels with compositions that approximate those in ordinary chondrites.

2. THEORETICAL APPROACH

Equilibrium between metal, a Pt-bearing alloy in our case, and a chromite-bearing spinel in the presence of an oxygen-bearing vapor can be represented by the reaction

$$Fe^{PtFeCr} + 2Cr^{PtFeCr} + 2O_2 = FeCr_2O_4^{spinel}, \quad (1a)$$

In Eqns. 1b and 1c,

$$K_1 = \exp[-\Delta G_1^\circ/RT] = \frac{a_{FeCr_2O_4}^{spinel}}{(a_{Fe}^{PtFeCr})(a_{Cr}^{PtFeCr})^2\,(f_{O_2})^2}, \quad (1b)$$

$$a_{FeCr_2O_4}^{spinel} = \exp[-\Delta G_1^\circ/RT]\,(a_{Fe}^{PtFeCr})(a_{Cr}^{PtFeCr})^2\,(f_{O_2})^2. \quad (1c)$$

a_i^j refers to the activity of component i in phase j, K_1 is the temperature-dependent equilibrium constant, R is the gas constant, T is the temperature in Kelvin, ΔG_1° is the free energy of formation of $FeCr_2O_4$ from the elements, and f_{O_2} is the oxygen fugacity. Eqn. 1c is the basis for our experimental approach to evaluating the thermodynamic properties of multicomponent spinels; i.e., given temperature, f_{O_2}, and ΔG_1°, Eqn. 1c yields the activity of chromite provided the activities of Fe and Cr in the metal are known. The thermodynamic properties of ternary Pt-Fe-Cr alloys, which are necessary to evaluate a_{Fe}^{PtFeCr} and a_{Cr}^{PtFeCr} in our experiments, have not been previously investigated, so we first performed a set of experiments to constrain activity–composition relationships in the relevant portion of this system.

Many binary systems of interest to metallurgists and geochemists are adequately described by expressing the excess free energy of mixing (ΔG^{ex}) as a Taylor expansion in composition, truncated after a suitable number of terms (e.g., Wohl, 1946, 1953). For many systems, a second or third order polynomial is adequate (e.g., Saxena, 1973; Grover, 1977), but where the two components are characterized by highly differing atomic or molecular size and/or shape, a fourth-order polynomial in terms of composition (sometimes referred to as a four-suffix asymmetric subregular solution) may be required leading to:

$$\frac{\Delta G^{ex}}{RT} = X_j^\phi X_i^\phi (X_j^\phi W_{ij} + X_i^\phi W_{ji} - X_j^\phi X_i^\phi D_{ji}). \quad (2)$$

In Eqn. 2, W_{ij} and D_{ij} are subregular interaction parameters (temperature- and composition-independent constants referred to as Margules parameters; Hildebrand, 1929), and X_i^ϕ is the mole fraction of component i in the solid solution ϕ. The activity of a particular component i, a_i^ϕ, is derived by differentiating the sum

$$\sum_j n_j\,\Delta G^{ex}$$

overall j with respect to the number of moles of component i, n_i. For a binary alloy, the activity coefficient, γ_i^ϕ (obtained through the identity $\gamma_i^\phi = a_i^\phi/X_i^\phi$) can be expressed as a function of composition according to

$$RT\ln\gamma_i^\phi = [W_{ji} + 2(W_{ij} - W_{ji} - D_{ji})\,X_i^\phi + 3D_{ji}(X_i^\phi)^2](X_j^\phi)^2. \quad (3)$$

Polynomial functions can also be constructed to represent the excess free energy of mixing in ternary and higher solutions. For example, Wohl (1953) expressed ΔG^{ex} as a power series truncated after the fourth degree and obtained a formulation in which the binaries have a four-suffix subregular behavior:

$$\frac{\Delta G^{ex}}{RT} = \sum_{i\neq j} X_i^\phi X_j^\phi (X_i^\phi W_{ij} + X_j^\phi W_{ij} - X_i^\phi X_j^\phi D_{ij}) + X_i^\phi X_j^\phi X_k^\phi \left(\tfrac{1}{2}\sum_{i\neq j} W_{ij} - \sum_{i\neq j} X_i^\phi C_i\right). \quad (4a)$$

Most of the terms in this equation refer to binaries (cf. Eqn. 2); the effects of ternary interactions are incorporated via the ternary interaction parameters, C_i's. Letting components 1 = Pt, 2 = Cr, and 3 = Fe and differentiating Eqn. 4a for ΔG^{ex} in the ternary system with respect to the number of moles of Cr results in the following expression (confirmed using Mathematica; Wolfram, 1999) for the activity coefficient of Cr (Wohl, 1953):

$$\begin{aligned} RT\ln\gamma_{Cr}^{PtFeCr} = {} & [W_{PtCr} + 2 \times (W_{CrPt} - W_{PtCr} - D_{PtCr}) \\ & \times X_{Cr}^{PtFeCr} \\ & + 3\,D_{PtCr}\,(X_{Cr}^{PtFeCr})^2]\,(X_{Pt}^{PtFeCr})^2 + [W_{CrFe} + 2 \\ & \times (W_{FeCr} - W_{CrFe} - D_{CrFe}) \times X_{Cr}^{PtFeCr} \\ & + 3\,D_{CrFe}\,(X_{Cr}^{PtFeCr})^2]\,(X_{Fe}^{PtFeCr})^2 \\ & + X_{Fe}^{PtFeCr} X_{Pt}^{PtFeCr} [\tfrac{1}{2}(W_{PtCr} + W_{CrPt} + W_{FeCr} \\ & + W_{CrFe} - W_{PtFe} - W_{FePt}) + X_{Cr}^{PtFeCr}(W_{CrPt} \\ & - W_{PtCr} + W_{FeCr} - W_{CrFe}) + (X_{Pt}^{PtFeCr} \\ & - X_{Fe}^{PtFeCr}(W_{FePt} - W_{PtFe}) + 3X_{Fe}^{PtFeCr} X_{Pt}^{PtFeCr} D_{PtFe} \\ & - X_{Cr}^{PtFeCr} C_{Cr} - (1 - 3X_{Cr}^{PtFeCr})(X_{Cr}^{PtFeCr} C_{Cr} \\ & + X_{Pt}^{PtFeCr} C_{Pt} + X_{Fe}^{PtFeCr} C_{Fe})]. \end{aligned} \quad (4b)$$

Expressions for the other components can be obtained by advancing the subscript of the parameters and variables of the equation in the order Pt→Cr, Cr→Fe, Fe→Pt. For Fe, this leads to

$$\begin{aligned} RT\ln\gamma_{Fe}^{PtFeCr} = {} & [W_{CrFe} + 2 \times (W_{FeCr} - W_{CrFe} - D_{CrFe}) \\ & \times X_{Fe}^{PtFeCr} + 3\,D_{CrFe}\,(X_{Fe}^{PtFeCr})^2]\,(X_{Cr}^{PtFeCr})^2 + [W_{FePt} \\ & + 2 \times (W_{PtFe} - W_{FePt} - D_{FePt}) \times X_{Fe}^{PtFeCr} \\ & + 3\,D_{FePt}\,(X_{Fe}^{PtFeCr})^2]\,(X_{Pt}^{PtFeCr})^2 \\ & + X_{Pt}^{PtFeCr} X_{Cr}^{PtFeCr} [\tfrac{1}{2}(W_{CrFe} + W_{FeCr} + W_{PtFe} \\ & + W_{FePt} - W_{CrPt} - W_{PtCr}) + X_{Fe}^{PtFeCr}(W_{FeCr} \\ & - W_{CrFe} + W_{PtFe} - W_{FeCr}) + (X_{Cr}^{PtFeCr} \\ & - X_{Pt}^{PtFeCr})(W_{PtCr} - W_{CrPt}) + 3X_{Pt}^{PtFeCr} X_{Cr}^{PtFeCr} D_{CrPt} \\ & - X_{Fe}^{PtFeCr} C_{Fe} - (1 - 3X_{Fe}^{PtFeCr})(X_{Fe}^{PtFeCr} C_{Fe} \\ & + X_{Cr}^{PtFeCr} C_{Cr} + X_{Pt}^{PtFeCr} C_{Pt})]. \end{aligned} \quad (4c)$$

Eqn. 3, 4b, and 4c are the tools with which we develop a ternary composition model for Pt-Fe-Cr alloys and evaluate activities of components in coexisting phases. The ternary is developed stepwise by first characterizing the three binaries, Pt-Fe, Pt-Cr, and Fe-Cr using Eqn. 3, and then evaluating the ternary interaction parameters via Eqn. 4b.

3. EXPERIMENTAL PROCEDURES AND ANALYTICAL TECHNIQUES

3.1. Analytical Procedures

Platinum alloys were analyzed for Pt, Fe, Cr, and Mg using a JEOL733 Superprobe with an accelerating voltage of 20 keV. Pure metals were used as standards for Pt, Fe, and Cr, and $MgAl_2O_4$ was used for Mg. With a beam current of 25 nA, counts were collected for 30 s on peak and 15 s at each background position on the standards. For the metals from the run products, Pt (L_α) and Fe (K_α) were analyzed first using the same analytical conditions as for the standards (i.e., 25 nA); Cr (K_α) and Mg (K_α) were then analyzed with beam currents as high as 400 nA and counting times of 10–30 min as needed to achieve detection limits $\leq$40 ppm for both Cr and Mg. Magnesium was found to be below detection limit in all alloys. Note that count rates on standards for Cr and Mg were much lower than on samples. This was necessary to prevent dead time corrections (which become nonlinear at very high count rates; J. Goldstein, personal communication, 1998) from introducing spurious counts. A ZAF correction procedure (Armstrong, 1988) was applied to the results.

Oxides (the various spinels and Cr_2O_3) were analyzed using an accelerating voltage of 15 keV and a beam current of 10 nA. X-ray counts were collected for 30 s on peak and 15 s on each background using Fe_2O_3, Cr_2O_3, and $MgAl_2O_4$ as standards.

3.2. Starting Materials

Chromite was prepared following the procedure of Petric and Jacob (1982): reagent grade powders of Fe (Alfa Products), Fe_2O_3 (JMC Puratronic), and Cr_2O_3 (JMC Puratronic) were ground in a molar ratio of 1:1:3 in an automated alumina mortar under ethanol for ~7 h. The mixture was pressed into 7 mm diameter pellets, placed inside loosely capped alumina ceramic cylinders, and sealed inside an evacuated quartz tube. The quartz tube was then heated at 1100°C for 4 d. Picrochromite was prepared following the procedure of O'Neill and Dollase (1994): reagent MgO (JMC Puratronic) was sintered in Al_2O_3 crucibles at 1000°C for 40 h and then ground together with reagent grade Cr_2O_3 in the required molar ratio in an automated alumina mortar under ethanol for ~6 h. The mixture was pressed into 13 mm diameter pellets, placed inside a Pt crucible, suspended from a sample holder at the hot spot of a vertical furnace, and held in a flowing H_2-CO_2 gas at 1100°C and $\log_{10} f_{O_2} = -11.5$ for 20 h. The above procedure was repeated twice to achieve complete conversion of the oxides to picrochromite. Chromite and picrochromite were mixed in three different ratios corresponding to nominal mole fractions of chromite, $X_{FeCr_2O_4}^{(Fe,Mg)Cr_2O_4}$, of 0.13, 0.46, and 0.83. The three spinel binary mixes and a pure chromite powder were each further mechanically mixed with 40 mol% Cr_2O_3 using an automated alumina mortar under ethanol for 2 h to produce starting materials for the experiments.

Homogeneity and the degree to which oxides were converted to chromite and picrochromite were determined using a Scintag Pad-V X-ray diffractometer and electron microprobe analyses. The average lattice parameter of five chromite syntheses is $a_o = 8.3665 \pm 0.0201$Å (1σ), consistent with a stoichiometric chromite standard, 8.3790Å (NBS 25,19,50). The average lattice parameter of two picrochromite syntheses was $a_o = 8.3240 \pm 0.0088$Å [reference standard taken as 8.3330Å (NBS 539,9,34)]. Some alumina was probably incorporated into the spinels and Cr_2O_3 during grinding in the alumina mortar. We can only place upper limits on this effect due to our use of alumina polishing compound but analyses of all run products [Cr_2O_3 (0.45 $\pm$ 0.16 wt% Al_2O_3), $FeCr_2O_4$ (0.32 $\pm$ 0.07 wt% Al_2O_3) and (Fe,Mg)Cr_2O_4 (0.68 $\pm$ 0.16 wt% Al_2O_3 excluding one sample with up to 2 wt% Al_2O_3 that we attribute to alumina grit)] show that the amounts of alumina in solid solution are small. Assuming that Raoult's law holds for the Cr-bearing oxides, these concentration levels introduce errors of 0.01–0.02% into Cr activity coefficients in alloys and 0.02–0.05% into calculated activity coefficients of $FeCr_2O_4$ spinels. These errors are small compared to other sources of error and we observed no correlation between apparent alumina content and the thermodynamic properties; consequently, we ignore the effects of alumina contamination on our results.

3.3. Experimental Conditions

Kessel et al. (2001) present a detailed description of our furnace setup and calibration procedures. All of the experiments were conducted at 1 atm in a Deltech DT-31 furnace or a home-built $MoSi_2$ furnace with gas-mixing capability. The oxygen fugacity was set by mixing CO_2 and H_2 gases and measured using an yttria-doped-zirconia solid electrolyte oxygen sensor ($SIRO_2$, Ceramic Oxide Fabricators, Ltd., Australia) with an uncertainty of $\pm$0.05 log units. Temperatures were measured using a Pt-$Pt_{90}Rh_{10}$ (type S) thermocouple and are estimated to be accurate to within $\pm$3°C. All experiments were conducted at 1300°C.

In each experiment, up to five crucibles, made from 0.625 cm diameter, 1 cm long Al_2O_3 rods (Vesuvius McDanel), were suspended using Pt wire from a sample holder in the vicinity of the furnace hot spot. Each crucible contained up to three horizontally stacked pellets (7 mm diameter, 1–2 mm thick) of identical oxide/s pressed around three pieces of Pt or Pt-Fe wire of known composition (see preparation procedures and compositions in Kessel et al., 2001). One crucible contained a pellet of Cr_2O_3 pressed around pure Pt wires [3–5 mm long, 75 μm diameter wires (99.9999%, Alfa ÆSAR)]. A second crucible contained one or more pellets of $FeCr_2O_4$ + Cr_2O_3, each pellet containing two wires of Pt-Fe alloy of known composition, above and below the expected equilibrium Fe concentration at the conditions of the experiment. Each of the remaining three crucibles contained pellets of one of the three spinel binary mixes [(Fe,Mg)Cr_2O_4 + Cr_2O_3] pressed around two Pt-Fe alloys.

Experiments were conducted for 8–14 d to achieve a close approach to equilibrium of the Pt-alloys with the surrounding oxides. These run durations were at least twice the characteristic time required to homogenize Fe in Pt wire based on the diffusion data of Berger and Schwartz (1978). We are not aware of any diffusion data on Cr in Pt, but concentrations of both Fe and Cr across the wires were homogeneous within analytical error. Also, the Pt-Fe wires of initially different compositions and in pellets at different positions in a stack converged in each crucible to compositions that were indistinguishable. Run durations were also found to be sufficient for complete conversion of the binary spinel mixtures to a homogeneous solid-solution phase as shown by EPMA analyses.

Experiments were terminated by raising the crucibles into the cold region of the furnace under the flowing gas mixture. Once cooled, samples were removed from the furnace. A small piece of each pellet containing a Pt-alloy surrounded by oxides was mounted in epoxy within a brass cylinder for examination of the textures around the wire and analyses of the oxides. The second wire from each pellet was physically separated from the adjacent oxides, mounted using epoxy to a piece of SiO_2 glass, and then mounted in epoxy within a brass cylinder such that a circular cross section of the wire was exposed. This sample was used to determine the alloy composition and to check for homogeneity across the wire. Alumina impregnated papers were used to expose the wires and oxides, and diamond powder ($<$0.25 μm) was used to prepare the final polished surfaces.

4. EXPERIMENTAL RESULTS

The experimental conditions and results for each set of experiments are listed in Tables 1 to 3. The experiments were conducted at 1300°C, with oxygen fugacities ranging from $\log_{10} f_{O_2} = -11.63$ to -7.90, corresponding to -0.86 log units below the iron–wüstite (IW) buffer to $+2.83$ log units above. Values of X_{Fe}^{PtFeCr} and X_{Cr}^{PtFeCr} were calculated from the measured wt% Fe and Cr by averaging all analyses (3–10) made on each wire. The averages and their uncertainties (the standard

Table 1. Experimental conditions and results for Pt/Cr + Cr_2O_3 at 1300°C.

Run	$\log_{10} f_{O_2}$ (atm)	Time (hr)	N[a]	X_{Cr}^{PtCr}[b]	$\ln\gamma_{Cr}^{PtCr}$[c]
RK281	−11.63	402	10	0.2386 (29)[d]	−6.06 (9)
RK191	−11.36	212.5	3	0.2130 (23)	−6.41 (9)
RK150	−11.07	284	7	0.1943 (10)	−6.82 (9)
RK135	−10.83	214	6	0.1639 (12)	−7.06 (9)
RK291	−10.68	236	3	0.1570 (20)	−7.29 (9)
RK255	−10.61	313	5	0.1610 (16)	−7.42 (9)
RK212	−10.17	211	5	0.1309 (28)	−7.98 (9)
RK286	−9.83	256	5	0.1040 (14)	−8.34 (9)
RK248	−9.67	216	10	0.0936 (35)	−8.50 (10)
RK137	−9.50	191	3	0.0799 (6)	−8.64 (9)
RK156	−9.25	189.5	3	0.0689 (9)	−8.94 (9)
RK267	−9.22	309.5	5	0.0679 (8)	−8.97 (9)
RK218	−8.73	330	10	0.0433 (22)	−9.36 (10)
RK296	−8.69	221.5	3	0.0396 (3)	−9.34 (9)
RK180	−7.90	188	4	0.0131 (3)	−9.60 (9)

[a] N = number of analyses.
[b] X_i^j = mole fraction of i in j.
[c] γ_i^j = activity coefficient of i in j.
[d] Numbers enclosed in parentheses indicate one standard deviation of the distribution calculated by error propagation.

deviation of the distribution of measured alloy compositions from each wire) are listed in the tables. Results for Pt-alloys equilibrated with Cr_2O_3 (Table 1) were used to constrain an activity–composition model for the Pt-Cr binary system. Compositions of Pt-alloys equilibrated with $FeCr_2O_4$ + Cr_2O_3 (Table 2) and (Fe,Mg)Cr_2O_4 + Cr_2O_3 (Table 3) were used to construct a ternary Pt-Fe-Cr model by taking advantage of the presence of Cr_2O_3 in the mixes, which together with the f_{O_2} fixed the activity of Cr in the alloy. Platinum-alloys equilibrated with $FeCr_2O_4$ + Cr_2O_3 were also used to evaluate the free energy of formation of end-member chromite and those equilibrated with (Fe,Mg)Cr_2O_4 + Cr_2O_3 to evaluate the thermodynamic properties of binary (Fe,Mg)Cr_2O_4 spinels.

4.1. Pt-Fe and Fe-Cr Binaries

Activity–composition relationships of alloys in the Pt-Fe system at various temperatures were evaluated in Kessel et al. (2001) and only a brief summary is presented here. At 1300°C, the system is characterized by strong negative deviations from ideality that can be described by a three-suffix asymmetric subregular solution with two binary interaction parameters (i.e., Eqn. 3 with $D_{ji} = 0$), values of which are listed in Table 4. The thermodynamic properties of alloys in the Fe-Cr system have little influence on our model for Pt-Fe-Cr alloys because this binary is much more ideal than either the Pt-Fe or Pt-Cr joins, leading to a small contribution to the activity coefficient, at least for compositions of interest for this study (i.e., very low in Cr and relatively rich in Pt). For the Fe-Cr binary, we used activity–composition relationships for Fe-Cr austenite (γ, fcc) alloys ($X_{Cr}^{FeCr} \leq 0.06$ at 1300°C) from Andersson and Sundman (1987). For consistency with Eqns. 3 and 4, we refit their model activities at 1300°C to a three-suffix asymmetric subregular solution with least-squares best-fit interaction parameters as given in Table 4. These alloys are characterized by a moderate positive deviation from ideality.

4.2. Pt-Cr Binary

Activity–composition relationships in the Pt-Cr system were determined following the approach used by Kessel et al. (2001)

Table 2. Experimental conditions and results for Pt/Fe + $FeCr_2O_4$ + Cr_2O_3 at 1300°C.

Run[a]	$\log_{10} f_{O_2}$ (atm)	Time (hr)	X_{Cr}^{PtFeCr}[b]	X_{Fe}^{PtFeCr} (initial)	X_{Fe}^{PtFeCr} (final)	$\ln\gamma_{Cr}^{PtFeCr}$[c] (observed)	$\ln\gamma_{Cr}^{PtFeCr}$ (model)	$\ln\gamma_{Fe}^{PtFeCr}$ (model)	ΔG_6^{o}[e] (kJ/mol)	ΔG_1^{o}[f] (kJ/mol)
RK280-43	−11.63	402	0.00462 (5)[d]	0.539	0.527 (3)	−2.12 (9)	−2.08 (3)	−1.47 (2)	−202.6 (8)	−922.8 (3.5)
RK190-38	−11.36	212.5	0.00427 (14)	0.477	0.499 (3)	−2.50 (10)	−2.41 (3)	−1.70 (3)	−202.4 (9)	−921.3 (3.6)
RK274-43	−11.20	431	0.00388 (8)	0.447	0.483 (4)	−2.68 (9)	−2.60 (5)	−1.85 (4)	−202.4 (9)	−921.8 (3.7)
RK205-28	−11.07	190	0.00347 (3)	0.524	0.467 (3)	−2.79 (9)	−2.81 (4)	−2.00 (3)	−202.8 (9)	−924.4 (3.5)
RK134-10	−10.83	214	0.00299 (12)	0.472	0.445 (3)	−3.05 (10)	−3.09 (4)	−2.22 (2)	−202.8 (9)	−924.9 (3.7)
RK134-21	−10.83	214	0.00298 (6)	0.539	0.444 (9)	−3.05 (9)	−3.11 (12)	−2.24 (6)	−203.1 (1.1)	−925.8 (4.5)
RK199-38	−10.73	189.5	0.00285 (11)	0.400	0.435 (4)	−3.19 (10)	−3.22 (5)	−2.33 (6)	−202.9 (1.1)	−924.9 (3.8)
RK290-28	−10.68	236	0.00244 (4)	0.524	0.431 (1)	−3.12 (9)	−3.27 (2)	−2.37 (3)	−202.8 (9)	−928.0 (3.4)
RK254-44	−10.61	313	0.00274 (4)	0.371	0.428 (6)	−3.35 (9)	−3.31 (7)	−2.40 (5)	−202.3 (1.0)	−922.4 (3.9)
RK211-30	−10.17	211	0.00209 (8)	0.400	0.389 (2)	−3.85 (10)	−3.85 (3)	−2.87 (4)	−203.0 (1.0)	−924.4 (3.6)
RK237-33	−10.00	642.5	0.00213 (21)	0.359	0.376 (2)	−4.16 (13)	−4.03 (4)	−3.02 (5)	−202.8 (1.0)	−920.6 (4.3)
RK285-33	−9.83	256	0.00150 (4)	0.359	0.369 (2)	−4.10 (9)	−4.14 (3)	−3.12 (4)	−201.9 (1.0)	−924.2 (3.6)
RK247-30	−9.67	216	0.00143 (3)	0.400	0.352 (2)	−4.32 (9)	−4.37 (3)	−3.34 (5)	−203.0 (1.1)	−925.7 (3.6)
RK136-9	−9.50	191	0.00127 (5)	0.361	0.343 (4)	−4.49 (10)	−4.51 (5)	−3.47 (7)	−202.5 (1.3)	−924.3 (3.9)
RK136-10	−9.50	191	0.00135 (7)	0.472	0.342 (2)	−4.56 (11)	−4.52 (4)	−3.48 (3)	−202.7 (9)	−923.1 (3.8)
RK136-11	−9.50	191	0.00133 (8)	0.275	0.343 (2)	−4.54 (11)	−4.51 (3)	−3.47 (3)	−202.5 (9)	−923.0 (3.8)
RK266-33	−9.22	309.5	0.00107 (7)	0.359	0.321 (1)	−4.82 (11)	−4.83 (2)	−3.78 (2)	−203.1 (9)	−924.7 (3.8)
RK232-39	−9.01	644	0.00111 (3)	0.352	0.309 (2)	−5.21 (10)	−5.01 (3)	−3.96 (3)	−202.9 (9)	−918.9 (3.6)
RK295-11	−8.69	221.5	0.00070 (3)	0.275	0.293 (3)	−5.31 (10)	−5.25 (4)	−4.20 (10)	−201.9 (1.6)	−921.5 (3.9)

[a] RKx-y: experiment #x with initial Pt-Fe alloy #y, y refers to the run in Kessel et al. (2001) in which the initial alloy was produced.
[b] X_i^j = mole fraction of i in j based on three analyses for Cr and five for Fe.
[c] γ_i^j = activity coefficient of i in j, model values calculated based on f_{O_2}, final X_{Fe}^{PtFeCr}, and $\Delta G^{\circ}_{f,\,Cr_2O_3}$ from Holzheid and O'Neill (1995).
[d] Numbers enclosed in parentheses indicate one standard deviation of the distribution calculated by error propagation.
[e] ΔG_i° free energy of formation of chromite for reaction i.
[f] Calculated directly from Eqn. 1.

Table 3. Experimental conditions and results for Pt/Fe + (Fe,Mg)Cr_2O_4 + Cr_2O_3 at 1300°C.

Run[a]	$\log_{10} f_{O_2}$ (atm)	Time (hr)	$X^{(Fe,Mg)Cr_2O_4}_{FeCr_2O_4}$	X^{PtFeCr}_{Cr}[b]	X^{PtFeCr}_{Fe} (initial)	X^{PtFeCr}_{Fe} (final)	$\ln\gamma^{PtFeCr}_{Cr}$[c] (observed)	$\ln\gamma^{PtFeCr}_{Cr}$ (model)	$\ln\gamma^{PtFeCr}_{Fe}$ (model)	$a^{(Fe,Mg)Cr_2O_4}_{FeCr_2O_4}$[e] (6a)	$a^{(Fe,Mg)Cr_2O_4}_{FeCr_2O_4}$ (1a)
RK147-9	−11.07	284	0.13	0.02395 (25)[d]	0.361	0.312 (3)	−4.72 (9)	−4.60 (4)	−3.58 (2)	0.14 (1)	0.17 (3)
RK147-11	−11.07	284	0.13	0.02571 (70)	0.275	0.307 (2)	−4.80 (9)	−4.64 (3)	−3.62 (2)	0.13 (1)	0.17 (3)
RK148-9	−11.07	284	0.46	0.00772 (3)	0.361	0.398 (1)	−3.59 (9)	−3.65 (2)	−2.69 (2)	0.43 (3)	0.37 (5)
RK148-11	−11.07	284	0.46	0.00748 (12)	0.275	0.403 (1)	−3.56 (9)	−3.58 (2)	−2.63 (2)	0.46 (3)	0.43 (6)
RK148-13	−11.07	284	0.46	0.00720 (4)	0.220	0.405 (2)	−3.52 (9)	−3.56 (3)	−2.61 (1)	0.47 (3)	0.42 (6)
RK149-9	−11.07	284	0.83	0.00423 (5)	0.361	0.455 (4)	−2.99 (9)	−2.94 (5)	−2.11 (3)	0.87 (6)	0.92 (16)
RK149-11	−11.07	284	0.83	0.00424 (1)	0.275	0.451 (3)	−2.99 (9)	−3.00 (3)	−2.15 (2)	0.82 (5)	0.79 (12)
RK149-13	−11.07	284	0.83	0.00432 (4)	0.220	0.452 (6)	−3.01 (9)	−2.98 (7)	−2.14 (4)	0.83 (6)	0.85 (17)
RK282-13	−9.83	256	0.13	0.00292 (1)	0.220	0.321 (1)	−5.41 (9)	−5.55 (2)	−4.53 (3)	0.19 (1)	0.14 (2)
RK282-44	−9.83	256	0.13	0.00252 (7)	0.371	0.329 (2)	−5.41 (9)	−5.57 (2)	−4.56 (2)	0.18 (1)	0.13 (2)
RK283-13	−9.83	256	0.46	0.00180 (4)	0.220	0.356 (2)	−4.77 (9)	−4.80 (2)	−3.75 (2)	0.49 (3)	0.45 (6)
RK283-44	−9.83	256	0.46	0.00179 (4)	0.371	0.357 (2)	−4.62 (9)	−4.69 (4)	−3.65 (3)	0.56 (4)	0.47 (8)
RK284-13	−9.83	256	0.83	0.00345 (10)	0.220	0.215 (2)	−4.28 (9)	−4.31 (3)	−3.28 (3)	0.88 (6)	0.81 (13)
RK284-44	−9.83	256	0.83	0.00407 (6)	0.371	0.206 (1)	−4.27 (9)	−4.29 (2)	−3.27 (3)	0.89 (6)	0.83 (13)
RK292-11	−8.69	221.5	0.13	0.00310 (3)	0.275	0.197 (2)	−6.79 (9)	−6.69 (3)	−5.84 (3)	0.14 (1)	0.17 (3)
RK292-36	−8.69	221.5	0.13	0.00309 (10)	0.211	0.194 (2)	−6.79 (10)	−6.72 (3)	−5.89 (4)	0.13 (1)	0.15 (2)
RK293-11	−8.69	221.5	0.46	0.00123 (3)	0.275	0.255 (1)	−5.87 (9)	−5.82 (2)	−4.82 (3)	0.50 (3)	0.53 (8)
RK293-36	−8.69	221.5	0.46	0.00122 (6)	0.352	0.253 (1)	−5.86 (10)	−5.84 (2)	−4.84 (4)	0.49 (3)	0.49 (9)
RK294-11	−8.69	221.5	0.83	0.00077 (2)	0.275	0.283 (2)	−5.41 (9)	−5.39 (3)	−4.36 (4)	0.88 (6)	0.88 (14)

[a] RKx-y: experiment #x with initial Pt-Fe alloy #y; y refers to the run in Kessel et al. (2001) in which the initial alloy was produced.
[b] X_i^j = mole fraction of i in j based on three analyses for Cr and five for Fe.
[c] γ_i^j = activity coefficient of i in j, model values calculated based on f_{O_2}, final X^{PtFeCr}_{Fe}, and $\Delta G^\circ_{f,Cr_2O_3}$ from Holzheid and O'Neill (1995).
[d] Numbers enclosed in parentheses indicate one standard deviation of the distribution calculated by error propagation.
[e] $a^{(Fe,\ Mg)Cr_2O_4}_{FeCr_2O_4}$ = activity of chromite as calculated from reaction 6a or 1a.

for Pt-Fe alloys. Initially pure Pt wire was equilibrated with Cr_2O_3 at a fixed temperature and f_{O_2}. Under these conditions, if the reaction

$$2Cr^{PtCr} + \tfrac{3}{2}O_2 = Cr_2O_3 \qquad (5a)$$

reaches equilibrium, the corresponding expression for the equilibrium constant can be solved for a^{PtCr}_{Cr}:

$$a^{PtCr}_{Cr} = \left(\frac{a^{oxide}_{Cr_2O_3}}{K_5 (f_{O_2})^{3/2}}\right)^{1/2}. \qquad (5b)$$

The equilibrium constant, K_5, can be obtained from the free energy of formation of Cr_2O_3 from the elements, ΔG°_5, via $\Delta G^\circ_5 = -RT\ln K_5$. We used ΔG°_5 from Holzheid and O'Neill (1995). Since Cr_2O_3 is essentially a stoichiometric oxide throughout the range of experimental conditions explored in this study (as expected from Kofstad, 1983, and confirmed by EPMA analyses), its activity, $a^{oxide}_{Cr_2O_3}$, is taken as equal to 1, and a^{PtCr}_{Cr} can be readily calculated from Eqn. 5b. Iron was detected in the Pt-Cr wires (presumably due to contamination by vapor transport from adjacent crucibles), but was always less than 0.4 wt% Fe. Such low Fe concentrations would introduce only a small error in the calculation of γ^{PtCr}_{Cr} (less than 0.3% based on the ternary model developed below).

Experimental run conditions are listed in Table 1. Uncertainties in $\ln\gamma^{PtCr}_{Cr}$ were found by propagating errors on temperature, $\log_{10} f_{O_2}$, and X^{PtCr}_{Cr} (<5%) to be less than 1.5%. Alloys in the Pt-Cr system are characterized by strong negative deviations from ideality (i.e., $\gamma^{PtCr}_{Cr} \ll 1$) over the range of compositions explored in this study. Figure 1 shows our data for $RT\ln\gamma^{PtCr}_{Cr}$ plotted against X^{PtCr}_{Cr} compared to the best fits assuming three-suffix and four-suffix subregular solution behavior. Our data are poorly fit by a three-suffix asymmetric subregular solution at the Cr-poor end of the binary but are well-described by a four-suffix solution. Uncertainties in the Margules parameters were calculated using a Monte Carlo simulation. Two sets of

Table 4. Recommended values of thermodynamic parameters.

Interaction parameter[a]	Value (kJ/mol)	1σ	Source[e]
	Alloys		
W_{PtFe}	−138.0	3.3	1
W_{FePt}	−90.8	23.9	1
D_{PtFe}	0.0		1
W_{PtCr}	−129.1	1.2	2
W_{CrPt}	−80.9	4.4	2
D_{PtCr}	+94.4	2.5	2
W_{CrFe}	+5.3		3
W_{FeCr}	+15.0		3
D_{FeCr}	0.0		3
C_{Cr}	0.0		2
C_{Pt}	+115.7		2
C_{Fe}	−68.6		2
	Oxides		
$\Delta G^{o\,b}_1$	−923.5	2.1	2
$\Delta H^{o\,c}_{298}$	−1438		2 + 5
ΔG^o_6	−202.7	0.4	2
$W_{(Fe,Mg)Cr_2O_4}$[d]	+2.14	0.62	2

[a] W_{ij}, W_{ji}, and D_{ij} are binary interaction parameters for the system i-j (cf. Eqn. 2) and C_k are ternary interaction parameters for the system Pt-Fe-Cr.
[b] ΔG°_i = free energy of formation of chromite from reaction i calculated directly via Eqn. 1.
[c] ΔH°_{298} = enthalpy of formation of chromite at 298 K (see text).
[d] $W_{(Fe,Mg)Cr_2O_4}$ = interaction parameter for the chromite–picrochromite spinel binary.
[e] 1 = Kessel et al. (2001), 2 = this work, 3 = Andersson and Sundman (1987), 4 = Holzheid and O'Neill (1995), 5 = Klemme et al. (2000).

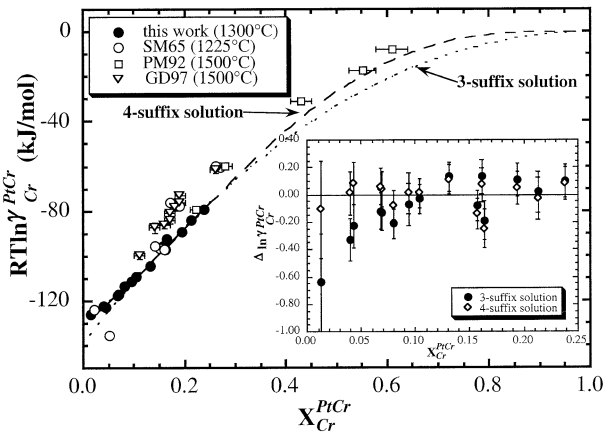

Fig. 1. Values of $RT\ln\gamma_{Cr}^{PtCr}$ vs. X_{Cr}^{PtCr} in the Pt-Cr system. The best fits to our data assuming four-suffix (solid curve, dashed where extended beyond our data) and three-suffix (dotted curve) asymmetric subregular solution behavior are shown. Literature data are from Schwerdtfeger and Muan (1965)—SM65; Pretorius and Muan (1992)—PM92; and Garbers-Craig and Dippenaar (1997)—GD97. Uncertainties (1σ) for both Pretorius and Muan (1992) and Garbers-Craig and Dippenaar (1997) were calculated by propagating reported uncertainties on alloy compositions given by Garbers-Craig and Dippenaar (1997). The inset shows deviations of the calculated $\ln\gamma_{Cr}^{PtCr}$ for each experiment from the best fits $\ln\gamma_{Cr}^{PtCr}$ calculated assuming three-suffix and four-suffix subregular solution models as a function of alloy composition. Uncertainties were calculated by propagating the uncertainties on the calculated $\ln\gamma_{Cr}^{PtCr}$.

10000 independent Excel-generated random numbers were used to recalculate the individual alloy composition and Cr activity for each experiment according to the uncertainties given in Table 1. For each recalculation of the composition and the activity of Cr in the alloy we used an iterative least-squares technique to find the binary interaction parameters best fitting all the experiments simultaneously. The average of the 10000 evaluated binary parameters and the standard deviations were determined and are given in Table 4. The required large D_{PtCr} value and the small uncertainty associated with it also indicate the necessity of using a four-suffix solution.

The deviations of our data from best fits to both models are shown as an inset in Figure 1 as a function of composition. Deviations from a four-suffix subregular solution model are independent of X_{Cr}^{PtCr} and most data plot within 1σ of the predicted curve. In contrast, deviations from the best fit to a three-suffix subregular solution model increase systematically with decreasing X_{Cr}^{PtCr}. Since $X_{Cr}^{PtCr} < 0.005$ for the ternary alloys in this study, we adopt the four-suffix subregular solution.

Results from previous studies at 1225 and 1500°C are also shown in Figure 1. For the sake of consistency, all of these data were recalculated using ΔG_5° from Holzheid and O'Neill (1995) based on the reported f_{O_2}, temperature, and alloy compositions. Schwerdtfeger and Muan (1965) equilibrated mixtures of Pt and Cr_2O_3 powders at 1225°C and known f_{O_2}'s and measured the Cr concentration in Pt by X-ray diffraction. Their results are scattered but generally consistent with our results at 1300°C. Pretorius and Muan (1992) and Garbers-Craig and Dippenaar (1997) equilibrated Pt wires with Cr_2O_3 at 1500°C and known f_{O_2}'s and measured the Cr concentration of the Pt alloys using SEM-EDS and EPMA, respectively. These two studies complement each other in alloy compositions and result in a well-defined trend displaced from our data. The results of these studies at 1500°C are not directly comparable to our 1300°C experiments, but all of their experiments yielded slightly Cr-poor alloys at any given f_{O_2} compared to predictions based on the subregular solution fit to our data (i.e., $RT\ln\gamma_{Cr}^{PtCr}$ is independent of temperature for a given alloy composition for such a solution). Such deviations would be consistent with incompletely equilibrated alloys, but both Pretorius and Muan (1992) and Garbers-Craig and Dippenaar (1997) demonstrated equilibrium through time series and reversal experiments. We have calculated uncertainties on $RT\ln\gamma_{Cr}^{PtCr}$ values for the results of Garbers-Craig and Dippenaar (1997) using their published uncertainties on alloy compositions (2%) and assuming that uncertainties in temperature and $\log_{10}f_{O_2}$ were comparable to those for our experiments (i.e., ± 3°C and ± 0.05). We used the same error estimates for data of Pretorius and Muan (1992) although analytical uncertainties are likely to be larger by several percent because they used SEM-EDS to determine alloy composition. Based on these calculated uncertainties, most of the data points from Garbers-Craig and Dippenaar (1997) and Pretorius and Muan (1992) are consistent at the 2σ level with an extrapolation of our model to 1500°C. Although most of these literature data cannot be distinguished from our data, if the systematic offset of the 1500°C data from our results is confirmed, it would suggest a more complex solution model (i.e., with temperature-dependent Margules parameters) than the subregular solution model we have utilized.

4.3. Pt-Fe-Cr Ternary Model

If Cr_2O_3 and an Fe-bearing oxide are equilibrated with Pt, the equilibrium Pt-bearing alloy will contain Fe and Cr, and although the activity of Cr in the alloy at a given f_{O_2} is fixed by the presence of Cr_2O_3 (as in the Pt-Cr_2O_3 experiments described in the preceding section), the Cr concentration will in general be different due to the presence of Fe. Table 2 presents results of a set of experiments in which Pt-alloys were equilibrated with mixtures of $FeCr_2O_4 + Cr_2O_3$. The equilibrium oxides were essentially end-member $FeCr_2O_4$ and Cr_2O_3, as confirmed by microprobe analyses of oxide grains in the vicinity of the Pt-alloys extracted from run products (i.e., the solubility of $FeCr_2O_4$, FeO, or Fe_2O_3 in Cr_2O_3 and vice versa are negligible over the range of conditions explored in this study). Moreover, Fe/(Cr + Fe) ratios of 0.326–0.335 in the $FeCr_2O_4$ correspond to mole fractions of Cr_3O_4 less than 0.023 and suggest essentially stoichiometric spinels with little or no Cr^{2+}. Table 3 presents results for a set of experiments in which Pt-alloys were equilibrated with mixtures of $(Fe,Mg)Cr_2O_4 + Cr_2O_3$. The addition of picrochromite to the spinel reduced the activity of FeO in the oxides relative to the $FeCr_2O_4 + Cr_2O_3$ assemblage, so the activity of Fe in the alloy at any given f_{O_2} is also reduced. Values of X_{Fe}^{PtFeCr} in our ternary experiments were in the range 0.19–0.53.

Alloy compositions (X_{Fe}^{PtFeCr} and X_{Cr}^{PtFeCr}) are shown in Figure 2 as a function of f_{O_2} for alloys in equilibrium with $FeCr_2O_4 + Cr_2O_3$. To test the approach to equilibrium, up to three pellets were placed in a crucible, each composed of the mixed oxides but pressed around Pt-Fe wires of different initial Fe content.

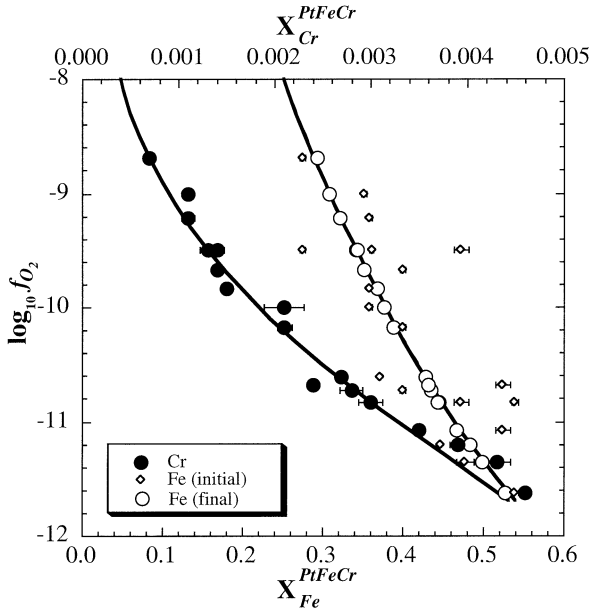

Fig. 2. X_{Fe}^{PtFeCr} (plotted along the lower x-axis) and X_{Cr}^{PtFeCr} (plotted along the upper x-axis) vs. $\log_{10} f_{O_2}$ in the Pt-Fe-Cr system for data obtained in this study. Small open diamonds are initial values of X_{Fe}^{PtFeCr} (Cr-free) of Pt-alloys in each pellet in a given experiment, and large circles represent the equilibrium alloy composition. Individual error bars (1σ) are plotted where larger than the symbol size. Also shown are predicted trends of $\log_{10} f_{O_2}$ as a function of X_{Fe}^{PtFeCr} and X_{Cr}^{PtFeCr} using the curve fit of our experimentally derived activities to a four-suffix Margules expansion (see text).

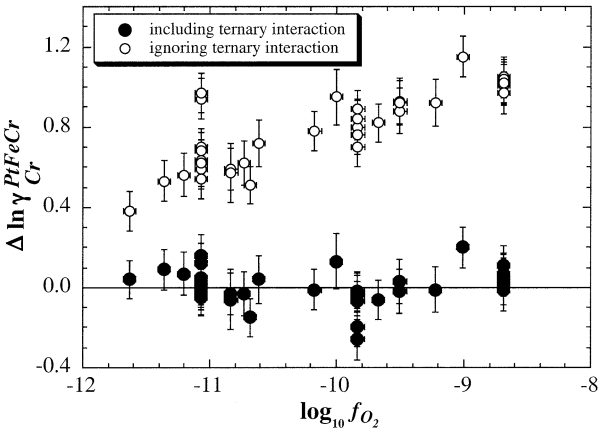

Fig. 3. Deviations between model values of $\ln\gamma_{Cr}^{PtFeCr}$ calculated using Eqn. 4b and experimentally observed values calculated via Eqn. 5b as a function of $\log_{10} f_{O_2}$. Filled symbols refer to values that include ternary interactions while open symbols refer to values in which ternary interactions are ignored. Error bars (1σ) are shown.

Starting with Pt-Fe alloys initially higher and lower in Fe than the equilibrium alloy composition enabled us to "reverse" our experimental results. The initial and final X_{Fe}^{PtFeCr} values of the alloys in each experiment are shown in Figure 2 and demonstrate that all Pt-alloys at a given f_{O_2} converged to the same Fe content within analytical errors. This convergence gives us considerable confidence that equilibrium was achieved in these experiments.

The activity of Cr in the Pt-alloys in equilibrium with either $FeCr_2O_4 + Cr_2O_3$ or $(Fe,Mg)Cr_2O_4 + Cr_2O_3$ was calculated using Eqn. 5b assuming that the Cr_2O_3 in equilibrium with the alloys was pure (i.e., $a_{Cr_2O_3}^{oxide} = 1$); corresponding values of $\ln\gamma_{Cr}^{PtFeCr}$ were obtained from the measured X_{Cr}^{PtFeCr}. For each of our 25 experiments, interaction parameters for the three bounding binaries (Table 4) and values of $\ln\gamma_{Cr}^{PtFeCr}$ were inserted into Eqn. 4b to produce one equation in the three unknown ternary parameters C_{Cr}, C_{Fe}, and C_{Pt}. We then used an iterative least-squares technique to find best-fit values of the three parameters. However, this resulted in a large value for C_{Cr} (on the order of 11000 kJ/mol) that led to inconsistencies in the binary spinel activity–composition relationships. The source of the problem is that C_{Cr} is multiplied by X_{Cr}^{PtFeCr} in Eqn. 4b, which has a very small value in our experiments, and therefore the value of C_{Cr} is poorly constrained. We found that fixing the value of C_{Cr} anywhere in the range of -500 to $+500$ kJ/mol and solving for the other two parameters (C_{Fe} and C_{Pt}) had little effect on the sum of the squares of the residuals of the model in the composition range covered by our experiments. We therefore chose arbitrarily to set C_{Cr} to 0 and determined best-fit values for the other two ternary interaction parameters in the Pt-Fe-Cr system. This procedure yielded $C_{Pt} = +115.7$ kJ/mol, and $C_{Fe} = -68.6$ kJ/mol (Table 4). Values of $\ln\gamma_{Cr}^{PtFeCr}$ calculated using Eqn. 4b and the best-fit interaction parameters are given in Tables 2 to 4. Uncertainties in the model $\ln\gamma_{Cr}^{PtFeCr}$ values calculated by propagating errors on temperature and alloy composition [X_{Cr}^{PtFeCr} (1–3%) and X_{Cr}^{PtFeCr} (0.1–3%)] are less then 2.5% (1σ). Deviations of model $\log_{10} f_{O_2}$ values calculated using Eqn. 5b from observed are shown in Figure 3 to be less than 0.2 log units. Deviations of model $\ln\gamma_{Cr}^{PtFeCr}$ that include ternary interactions are all within 2σ of observed values and are independent of $\log_{10} f_{O_2}$ (Fig. 3). In contrast, as shown in Figure 3, model $\ln\gamma_{Cr}^{PtFeCr}$ values in which ternary interactions are ignored yield much larger deviations and show a systematic increase with $\log_{10} f_{O_2}$, indicating that the ternary interaction effect is significant and can not be ignored.

The effect of Fe on Cr activity coefficients is significant and our model quantifies this. Figure 4a shows model values of $\ln\gamma_{Cr}^{PtFeCr}$ calculated using Eqn. 4b with the parameters from Table 4 as a function of X_{Cr}^{PtFeCr}. At constant X_{Cr}^{PtFeCr}, $\ln\gamma_{Cr}^{PtFeCr}$ increases with increasing Fe by 6 ln units for X_{Fe}^{PtFeCr} ranging from zero (i.e., Pt-Cr alloys) to 0.4. Also shown in Figure 4a are the model $\ln\gamma_{Cr}^{PtFeCr}$ values calculated for our experiments from the measured X_{Cr}^{PtFeCr} and ternary model parameters. The corresponding X_{Fe}^{PtFeCr} value for each Pt-alloy is shown next to the symbol. Model $\ln\gamma_{Fe}^{PtFeCr}$ values calculated from Eqn. 4c, essentially identical to values calculated using the Pt-Fe activity–composition model developed by Kessel et al. (2001), are given in Tables 2 and 3 together with calculated uncertainties. Uncertainties in model $\ln\gamma_{Fe}^{PtFeCr}$ calculated by propagating errors on temperature and alloy composition are less than 2.5% (1σ). The values of $\ln\gamma_{Fe}^{PtFeCr}$ are insensitive to whether or not ternary interactions are incorporated because $X_{Fe}^{PtFeCr} \gg X_{Cr}^{PtFeCr}$, and using either the best-fit C_i's or setting them equal to zero yields essentially the same results. This is demonstrated in Figure 4b showing model values of $\ln\gamma_{Fe}^{PtFeCr}$ calculated using Eqn. 4c as a function of X_{Fe}^{PtFeCr} for a range of X_{Cr}^{PtFeCr}. The model values of $\ln\gamma_{Fe}^{PtFeCr}$ calculated for our experiments are also shown and the corresponding X_{Cr}^{PtFeCr} value is given.

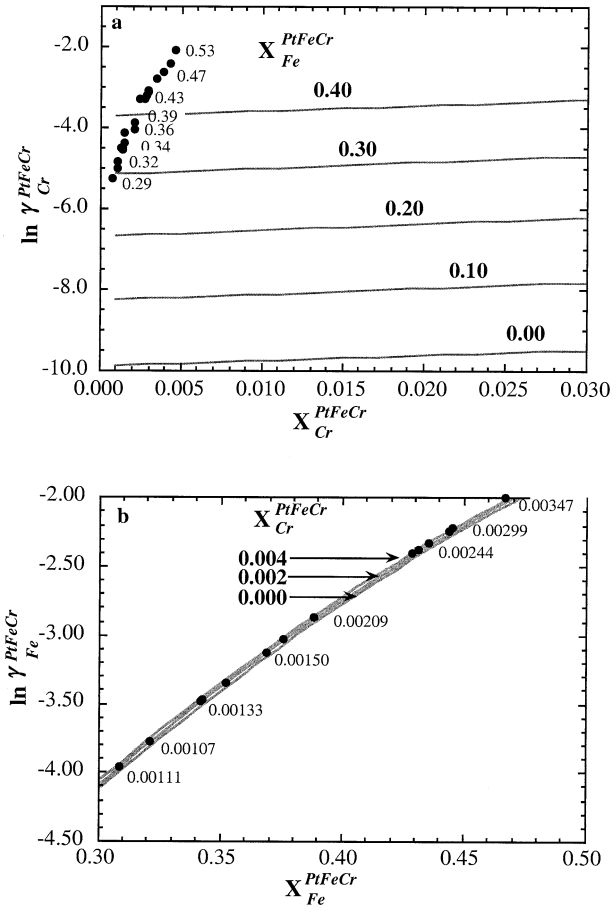

Fig. 4. (a) Model values of $\ln\gamma^{PtFeCr}_{Cr}$ as a function of X^{PtFeCr}_{Cr} calculated for various values of X^{PtFeCr}_{Fe}. Solid circles represent the model $\ln\gamma^{PtFeCr}_{Cr}$ values obtained in our experiments from the measured X^{PtFeCr}_{Cr}. Numbers adjacent to the symbols represent the corresponding X^{PtFeCr}_{Fe} values. (b) Model values of $\ln\gamma^{PtFeCr}_{Fe}$ as a function of X^{PtFeCr}_{Fe} calculated for various values of X^{PtFeCr}_{Cr}. Solid circles represent the model $\ln\gamma^{PtFeCr}_{Fe}$ values obtained in our experiments from the measured X^{PtFeCr}_{Fe}. Numbers adjacent to the symbols represent the corresponding X^{PtFeCr}_{Cr} values.

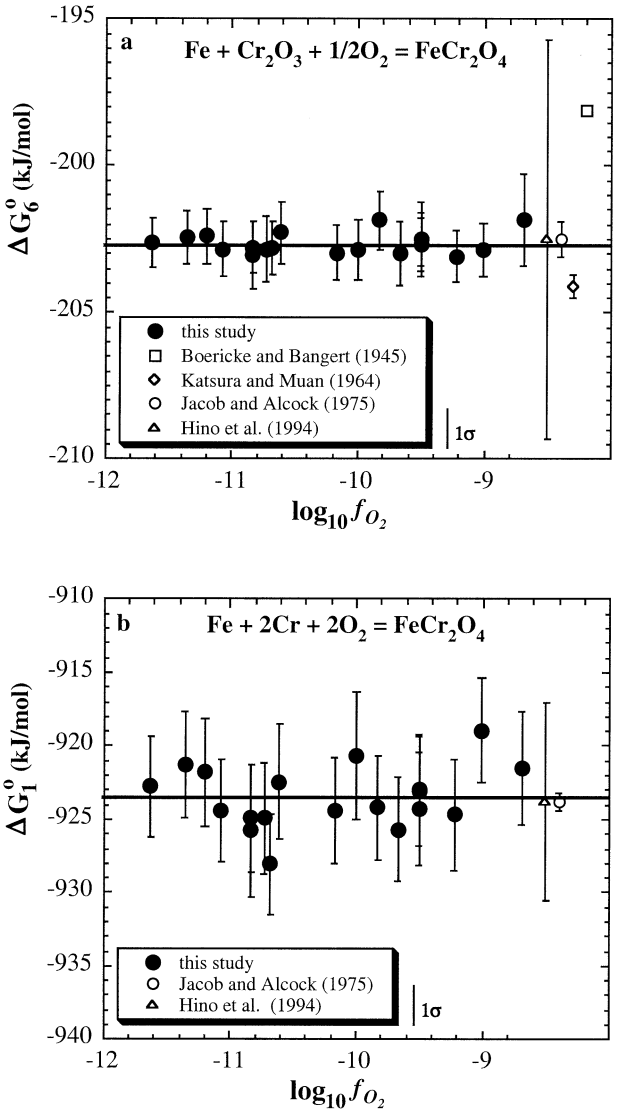

Fig. 5. Free energy of formation of $FeCr_2O_4$ at 1300°C as a function of $\log_{10} f_{O_2}$. Error bars (1σ) are shown. (a) Formation of $FeCr_2O_4$ from Cr_2O_3 and Fe and O_2 (Eqn. 6a) calculated using the model values of a^{alloy}_{Fe}. (b) Formation of $FeCr_2O_4$ from the elements (Eqn. 1a) calculated using the model values of a^{alloy}_{Cr} and a^{alloy}_{Fe}. Averages and 1σ values for Boericke and Bangert (1945), Katsura et al. (1975), Jacob and Alcock (1975), and Hino et al. (1994) are also shown (open symbols at right end of x-axis).

We conclude based on Figures 3 and 4 that the activities of Cr and Fe in Pt-alloys can be calculated for a given alloy composition using the model developed above. In the remainder of this paper, we use values of a^{PtFeCr}_{Cr} and a^{PtFeCr}_{Fe} calculated in this way to constrain the thermodynamic properties of chromite and chromite–picrochromite using Pt-alloy equilibration. The same approach could be used more generally to obtain activities of Cr- and Fe-bearing oxides and silicates and our original motivation for this study was to apply this model to the evaluation of chromite activities

4.4. Free Energy of Formation of Chromite

In the set of experiments in which Pt-alloys were equilibrated with mixtures of end-member $FeCr_2O_4$ and Cr_2O_3, equilibrium 1a holds, but the presence of Cr_2O_3 also allows an evaluation of the free energy of formation of chromite, ΔG°_6, from Cr_2O_3, Fe, and O_2 based on the equilibrium

$$Fe^{PtFeCr} + Cr_2O_3 + \frac{1}{2}O_2 = FeCr_2O_4^{spinel}. \quad (6a)$$

This yields and expression for ΔG°_6:

$$\Delta G^\circ_6 = -RT\ln\left[\frac{a^{spinel}_{FeCr_2O_4}}{a^{PtFeCr}_{Fe}\,(a^{oxide}_{Cr_2O_3})\,(f_{o_2})^{1/2}}\right]. \quad (6b)$$

Using our measured values of X^{PtFeCr}_{Fe} for each experiment, calculating a^{PtFeCr}_{Fe} from our activity–composition model for ternary alloys, and setting both $a^{spinel}_{FeCr_2O_4}$ and $a^{oxide}_{Cr_2O_3}$ equal to 1 allows ΔG°_6 to be determined from Eqn. 6b. Calculated values of ΔG°_6 are given in Table 2 and shown in Figure 5a as a

function of $\log_{10} f_{O_2}$. The uncertainties obtained by propagating errors on temperature, f_{O_2}, and a_{Fe}^{PtFeCr} are less than 1.5% (1σ). The average ΔG_6° and standard deviation of the mean at 1300°C is -202.7 ± 0.4 kJ/mol (Table 4), with no observed dependence on $\log_{10} f_{O_2}$.

Our results (Fig. 5a) differ from the values of -204.1 ± 0.4 kJ/mol and -198.1 kJ/mol obtained by Katsura and Muan (1964) and Boericke and Bangert (1945), respectively (Fig. 5a). In both studies, chromite was equilibrated with Fe metal and Cr_2O_3 using a gas-equilibrium method. However, as pointed out by Klemme et al. (2000), the equilibrium f_{O_2} for the assemblage chromite + Cr_2O_3 + Fe is so reducing that significant amounts of Cr^{2+} can be stabilized in the spinel. If this effect is ignored, substantial errors can be introduced in calculated free energies of reaction. For example, at 1600°C, $X_{FeCr_2O_4}^{spinel}$ in equilibrium with liquid iron and Cr_2O_3 is only 0.67 with $a_{FeCr_2O_4}^{spinel} = 0.69$ (Toker et al., 1991). This leads to an error of 4.7 kJ/mole in ΔG_6° if Cr^{2+} is ignored and an activity of unity for $a_{FeCr_2O_4}^{spinel}$ assumed in Eqn. 6b. The effect is likely to be smaller at lower temperatures unless the solid solution becomes strongly nonideal because the solubility of Cr^{2+} in metal-saturated chromite decreases with decreasing temperature (Toker et al., 1991). Katsura et al. (1975) found $X_{FeCr_2O_4}^{spinel} = 0.91$ at 1300°C for chromite in equilibrium with Fe metal and Cr_2O_3. If $a_{FeCr_2O_4}^{spinel} \sim X_{FeCr_2O_4}^{spinel}$ as is the case at 1600°C, then an error of 1.2 kJ/mole would be introduced into the inferred value of ΔG_6° due to the nonstoichiometry. Thus, much of the ~2 kJ/mole discrepancy between our inferred value for ΔG_6° at 1300°C and that obtained by Katsura and Muan (1964) may be due to the presence of divalent Cr in their chromites. However, deviations due Cr^{2+} are in the wrong direction to account for the difference between our result and ΔG_6° obtained by Boericke and Bangert (1945). We have no specific explanation for this discrepancy. We do note, however, that $\log_{10}(P_{H_2O}/P_{H_2})$, where P_i is the partial pressure of gaseous species i, is a quadratic function of 1/T for their data. A linear relationship would be expected given the 120°C range of their experiments and we therefore suspect that the study of Boericke and Bangert (1945) suffers from some unknown experimental problem. Regardless of the full explanations of the discrepancies between these older results from the literature and our data, the stabilization of Cr^{2+} in chromite under highly reducing conditions adds considerable complexity to the calculation of ΔG_6° based on the results of experiments conducted under highly reducing conditions. In this respect, the Pt-alloy equilibration technique utilized in this paper is preferable because the spinel is essentially stoichiometric $FeCr_2O_4$ (see section 4.3) under the relatively oxidizing conditions of our experiments.

Our results are indistinguishable from the values of $\Delta G_6^\circ = -202.5 \pm 6.8$ and -202.5 ± 0.6 kJ/mol obtained by Hino et al. (1994) and Jacob and Alcock (1975), respectively. Hino et al. (1994) equilibrated liquid silver with crucibles made of $FeCr_2O_4$ saturated with Cr_2O_3 at temperatures of 1150–1450°C and $\log_{10} f_{O_2}$ between -9.68 and -6.07 (3.0–4.5 log units above IW). The free energy of chromite was determined using their activity–composition model for Fe-Ag liquids. Jacob and Alcock (1975) determined the free energy of formation of chromite at temperatures between 750 and 1600°C and $\log_{10} f_{O_2}$ corresponding to the equilibrium of $FeCr_2O_4$ + Cr_2O_3 + Fe using thoria-bearing bielectrolyte solid-state galvanic cells based on Eqn. 6a. As noted by Klemme et al. (2000), earlier determinations of ΔG_6° using unprotected yttria- or calcia-stabilized-zirconia electrolytes (e.g., Tretjakov and Schmalzried, 1965) are not reliable due to electronic conductivity. The use of the more appropriate yttria-doped thoria bielectrolyte and the internally consistent results obtained by Jacob and Alcock (1975) suggest that equilibrium was reached during their experiments. The excellent agreement between our value and those of Hino et al. (1994) and Jacob and Alcock (1975) determined using entirely independent techniques provides strong validation of the activity–composition relationship for binary Pt-Fe alloys we have developed (Kessel et al., 2001) and of our conclusion that at low Cr concentrations in the alloys, the effects of Cr on Fe activity coefficients can be neglected.

The free energy of formation of $FeCr_2O_4$ from the elements, ΔG_6°, at 1300°C and 1 bar can be calculated from our alloy compositions. The measured values of X_{Fe}^{PtFeCr} and X_{Cr}^{PtFeCr} can be used given our activity–composition relationship for the ternary alloys to compute values of a_{Fe}^{PtFeCr} and a_{Cr}^{PtFeCr}, which can then be substituted into Eqn. 1b to calculate ΔG_6° directly. The observed values (Table 2) are independent of $\log_{10} f_{O_2}$ (Fig. 5b); the average and standard deviation of the mean at 1300°C is -923.5 ± 2.1 kJ/mol (Table 4). Alternatively, our values of ΔG_6° (Fig. 5a), can be corrected to ΔG_1° via ΔG_5° from Holzheid and O'Neill (1995), yielding -924.0 ± 0.4 kJ/mol. The same procedure, applied to ΔG_6° values of Hino et al. (1994) and Jacob and Alcock (1975), gives -923.8 ± 6.8 and -923.8 ± 0.6 kJ/mol, respectively. These four values of ΔG_6° at 1300°C are in excellent agreement at the 1σ level. Note that in contrast to ΔG_6°, our error on a direct determination ofΔG_1° is larger than that of Jacob and Alcock (1975) or our own value obtained via ΔG_6° and ΔG_5° because the direct determination of ΔG_1° requires an explicit evaluation of a_{Cr}^{PtFeCr}, which contributes uncertainty to the value of ΔG_1°. However, the fact that the determination of ΔG_1° based on our measured values of X_{Fe}^{PtFeCr} and X_{Cr}^{PtFeCr} is indistinguishable from values based on independent measurements and/or calculations from the literature provides support of the activity–composition relationship for ternary Fe-Pt-Cr alloys we have developed.

Our value of the free energy of formation of $FeCr_2O_4$ from the elements, ΔG_1°, at 1300°C and 1 bar allows us to calculate the enthalpy of formation at 298 K, ΔH_{298}°, given temperature-dependent heat capacity equations and a value for ΔS_{298}°, the entropy of formation of $FeCr_2O_4$ from the elements at 298K. Combining our value of $\Delta G_1^\circ = -923.5 \pm 2.1$ kJ/mol with heat capacities and third law entropies from Klemme et al. (2000) yields $\Delta H_{298}^\circ = -1438$ kJ/mol. A similar calculation using the compilation of Robie et al. (1978) leads to $\Delta H_{298}^\circ = -1452$ kJ/mol, reflecting a significantly lower ΔS_{298}°, which they adopted from Shomate (1944). Since Klemme et al. (2000) have shown that the measurements of Shomate (1944) do not include significant low temperature contributions to the heat capacity and hence ΔS_{298}°, the value of ΔH_{298}° derived using data from Klemme et al. (2000) is to be preferred. Our value of $\Delta H_{298}^\circ = -1438$ kJ/mol is somewhat more negative than the -1433 kJ/mol calculated by Klemme et al. (2000) and more positive than the -1445 kJ/mol used by Sack and Ghiorso (1991a). In the absence of high temperature heat of solution data, which is generally used to derive accurate values of ΔH_{298}°, we suggest that $\Delta H_{298}^\circ = -1438$ kJ/mol together with

thermochemical data in Klemme et al. (2000) be used to calculate the thermodynamic properties of stoichiometric $FeCr_2O_4$ as a function of temperature.

5. ACTIVITY OF CHROMITE IN (Fe,Mg)Cr_2O_4 SPINELS

In section 4, we presented a ternary model for Pt-Fe-Cr alloys using experiments in which (Fe,Mg)Cr_2O_4 + Cr_2O_3 were equilibrated with Pt-Fe-Cr alloys. We used the binary spinels primarily as a vehicle to extend the range of alloy compositions explored in this study by decreasing the activity of $FeCr_2O_4$ in the spinels (and that of Fe in the metal relative to coexistence with $FeCr_2O_4$ + Cr_2O_3 at a given f_{O_2}). However, these experiments also constrain the thermodynamic properties of binary (Fe,Mg)Cr_2O_4 spinels, and we examine these constraints in this section. As described above, three different mixes of $FeCr_2O_4$ + $MgCr_2O_4$ were studied experimentally (nominal mixes, expressed as mole fractions of $FeCr_2O_4$ in $Fe_XMg_{1-X}Cr_2O_4$ were $X^{(Fe,Mg)Cr_2O_4}_{FeCr_2O_4}$ = 0.13, 0.46, and 0.83), each mixed together with 40 mole% of Cr_2O_3. Up to three pellets of a given binary spinel mix were pressed around Pt-Fe wires, each with a different initial Fe content so that the equilibrium alloy composition could be approached from both Fe-poor and Fe-rich compositions. Homogeneous spinel and Cr_2O_3 were present in all run products as confirmed, with particular attention to the vicinity of the Pt-Fe alloys, by electron probe analyses. Analyzed values of $X^{(Fe,Mg)Cr_2O_4}_{FeCr_2O_4}$ in Cr_2O_3-saturated run products (calculated on an Al_2O_3-free basis) were 0.12 ± 0.01 (n = 12), 0.44 ± 0.05 (n = 18), and 0.81 ± 0.02 (n = 18), in agreement within uncertainties with the nominal values. The standard deviations refer to the distribution of measured spinel compositions and arise primarily from contamination via overlap of the beam on adjacent Cr_2O_3 grains during the analyses of individual spinel grains. The fraction of Fe^{3+} in the spinel run products, calculated assuming mass and charge balance, was found to be less than 0.001, and the coexisting Cr_2O_3 was found to be stoichiometric, indicating that the solubilities of Fe_3O_4 in $Fe_XMg_{1-X}Cr_2O_4$ and of FeO or Fe_2O_3 in Cr_2O_3 are negligible under the experimental conditions used in this study. (Fe + Mg)/(Cr + Fe + Mg) ratios of 0.324–0.340 were determined in the (Fe,Mg)Cr_2O_4, corresponding to less than 0.029 mole fraction of Cr_3O_4, suggesting a virtually stoichiometric spinel with little or no Cr^{2+}.

The activity of $FeCr_2O_4$ in $Fe_XMg_{1-X}Cr_2O_4$, $a^{(Fe,Mg)Cr_2O_4}_{FeCr_2O_4}$, can be calculated based on Eqn. 6b given the Fe content of the coexisting alloy at a given f_{O_2}. For each experiment, we substituted ΔG°_6 from Table 4 and a^{PtFeCr}_{Fe} calculated using Eqn. 4c into Eqn. 6b to obtain $a^{(Fe,Mg)Cr_2O_4}_{FeCr_2O_4}$. The calculated activities are given in Table 3 and shown in Figure 6 as a function of composition. Errors (1σ) on $a^{(Fe,Mg)Cr_2O_4}_{FeCr_2O_4}$ calculated using Eqn. 6a are 6–7% based on propagating the errors on temperature, f_{O_2}, and alloy composition. (Fe,Mg)Cr_2O_4 spinels are essentially ideal at 1300°C (Fig. 6). Our activities can be reasonably fit to a one-site symmetric regular solution of the form:

$$RT\ln\gamma^{(Fe,Mg)Cr_2O_4}_{FeCr_2O_4} = W_{(Fe,Mg)Cr_2O_4}\,(X^{(Fe,Mg)Cr_2O_4}_{MgCr_2O_4})^2, \qquad (7)$$

and a best fit of our data yields $W_{(Fe,Mg)Cr_2O_4}$ = +2.14 ± 0.62 kJ/mol (1σ) taking into account the uncertainties on $RT\ln\gamma^{(Fe,Mg)Cr_2O_4}_{FeCr_2O_4}$. The activities derived at $\log_{10}f_{O_2} = -9.83$ are systematically higher than the activities derived at either

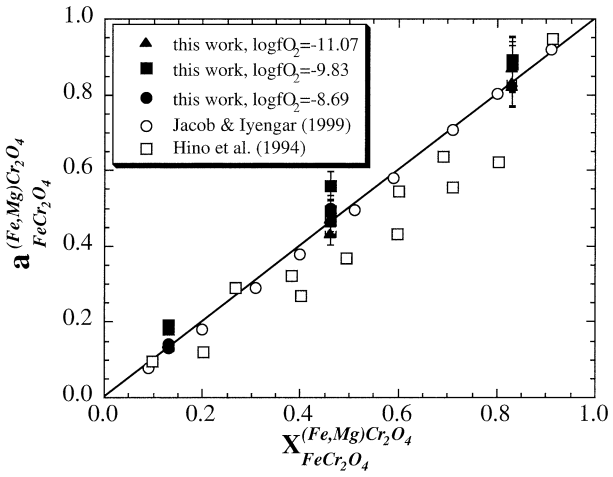

Fig. 6. $a^{(Fe,Mg)Cr_2O_4}_{FeCr_2O_4}$ at 1300°C as a function of $X^{(Fe,Mg)Cr_2O_4}_{FeCr_2O_4}$. Activities of chromite were calculated from reaction 6a based on the model a^{alloy}_{Fe}. Also shown are results from Hino et al. (1994) and Jacob and Iyengar (1999). Ideal solution behavior is indicated by the solid line.

$\log_{10}f_{O_2} = -11.07$ or -8.69 for reasons that are unclear, but all results agree within 2σ and a best fit excluding data obtained at $\log_{10}f_{O_2} = -9.83$ yields essentially ideal behavior ($W_{(Fe,Mg)Cr_2O_4}$ = +0.29 ± 0.75 kJ/mol). Also shown in Figure 6 are results at 1300°C from previous studies (Hino et al., 1994; Jacob and Iyengar, 1999). For consistency, previous results were recalculated based on the reported f_{O_2}, temperature, and spinel composition, using our ΔG°_6. Previous results for (Fe,Mg)Cr_2O_4 range from nearly ideal (Jacob and Iyengar, 1999) to systematic negative deviations from ideality (Hino et al., 1994). Hino et al. (1994) equilibrated liquid silver with crucibles made of (Fe,Mg)Cr_2O_4 saturated with Cr_2O_3 at temperatures between 1150 and 1450°C and $\log_{10}f_{O_2}$ between −7.73 and −6.20. Values of $a^{(Fe,Mg)Cr_2O_4}_{FeCr_2O_4}$ were then calculated using Eqn. 6b based on their experimentally determined activity–composition relationships for Fe-Ag liquids and their derived free energy of formation of $FeCr_2O_4$ from Fe and Cr_2O_3. Jacob and Iyengar (1999) determined $a^{(Fe,Mg)Cr_2O_4}_{FeCr_2O_4}$ at temperatures between 777 and 1077°C and $\log_{10}f_{O_2}$ corresponding to the equilibrium of $FeCr_2O_4$ + Cr_2O_3 + Fe using a bielectrolyte solid-state galvanic cell based on Eqn. 6a. Since both Fe and Cr_2O_3 exist as end-member phases in the cell, the activity of chromite is a function of the oxygen fugacity and the equilibrium constant at each temperature. They found no temperature dependence for the mixing properties of spinel and the activity of $FeCr_2O_4$ from their study presented in Figure 6 is an extrapolation of their data to 1300°C. Both data sets imply small negative deviations from ideality with the data of Hino et al. (1994) displaying greater deviations (recalculated using our ΔG°_6 to $W_{(Fe,Mg)Cr_2O_4}$ = −5.14 ± 2.22 kJ/mol) than those of Jacob and Iyengar (1999) (recalculated $W_{(Fe,Mg)Cr_2O_4}$ = −1.96 ± 0.09 kJ/mol). Despite the small and at present unexplained differences between the three studies compared in Figure 6, we conclude based on our own data and those from the literature that the absolute value of $W_{(Fe,Mg)Cr_2O_4}$ is not more than a few kilojoules and that spinels in the (Fe,Mg)Cr_2O_4 system are approximately ideal at 1300°C.

Chromite and picrochromite are end-member spinels with a

common trivalent cation, Cr^{3+}. Both spinels are overwhelmingly "normal" even at high temperature due to a large octahedral site preference energy for Cr^{3+} (−158 kJ, Dunitz and Orgel, 1957) compared to those of Mg^{2+} and Fe^{2+} (∼−17 kJ), leading to essentially exclusive occupation of the octahedral sites by Cr^{3+} (O'Neill and Dollase, 1994). Given this, in the absence of redox reactions, a large size mismatch between cations on the same site, or substitution of cations on multiple crystallographically distinct sites, the thermodynamic behavior of $(Fe,Mg)Cr_2O_4$ is influenced primarily by simple mixing of divalent cations on the tetrahedral site. The free energy of mixing in such simple spinel systems has been shown previously to approximate closely statistically ideal mixing (O'Neill and Navrotsky, 1984). Essentially ideal behavior or slightly positive deviations from ideality such as we have observed for $FeCr_2O_4$-$MgCr_2O_4$ solid solutions is also typical of other systems such as $FeSiO_3$-$MgSiO_3$ (e.g., Nafziger, 1973) where changes in composition involve only mixing of Fe^{2+} and Mg^{2+} on one site.

An alternative approach to calculating the activity of $FeCr_2O_4$ in $Fe_xMg_{1-x}Cr_2O_4$ solutions is based on the equilibrium between the spinel of interest and the Pt alloy (Eqn. 1a): That is, a_{Cr}^{PtFeCr} is not assumed to be fixed by f_{O_2} and the presence of Cr_2O_3 in the equilibrium assemblage; it is instead calculated from the measured X_{Cr}^{PtFeCr} and our activity–composition model (Eqn. 4b and the parameters listed in Table 4) for ternary alloys. The activity of $FeCr_2O_4$ in the three binary spinels in each experiment can then be calculated according to Eqn. 1c using the above determined ΔG_1°. Activities of chromite in $(Fe,Mg)Cr_2O_4$ calculated in this way and associated uncertainties (14–20%) obtained through propagation of errors on temperature, f_{O_2}, and alloy composition, are given in Table 3. Uncertainties in $a_{FeCr_2O_4}^{(Fe,Mg)Cr_2O_4}$ values calculated using this approach are much larger than activities calculated via Eqn. 6a due to relatively large uncertainties in a_{Cr}^{PtFeCr}. Differences in $a_{FeCr_2O_4}^{(Fe,Mg)Cr_2O_4}$ determined with these two methods are as much as 30%, but the approach of using Eqn. 1a is, nevertheless, potentially valuable in that it does not require the presence of Cr_2O_3, and thus extends the range of conditions under which spinel activities can be determined using our techniques. We conclude that Eqn. 1a provides a viable method for obtaining chromite activities where end-member Cr_2O_3 is not stable (although it is less precise than the method based on Cr_2O_3-saturated experiments).

6. CONCLUSIONS

The experimental technique developed in this study provides a method for obtaining chromite activities in multicomponent spinels by equilibrating the spinel of interest with Pt-alloy at a known temperature and oxygen fugacity. In particular, given the temperature and f_{O_2} of the experiment and the free energy of formation of chromite from the elements, the activity of chromite in any spinel can be determined if the activities of Fe and Cr in the Pt-alloy are known.

The activity–composition relationships in the ternary Pt-Fe-Cr system, modeled as a four-suffix asymmetric regular solution, were constrained by combining interaction parameters for the three bounding binaries with three ternary interaction parameters. The Pt-Cr binary is characterized by an asymmetric regular solution with three binary interaction parameters of $W_{PtCr} = -129.1 \pm 1.2$ kJ/mol, $W_{CrPt} = -80.9 \pm 4.4$ kJ/mol, and $D_{PtCr} = +94.4 \pm 2.5$ kJ/mol (1σ). Combining the thermodynamic properties of the Pt-Cr system with those of Pt-Fe (Kessel et al., 2001) and Fe-Cr (Andersson and Sundman, 1987), the ternary interaction parameters were found to be $C_{Pt} = +115.7$ kJ/mol and $C_{Fe} = -68.6$ kJ/mol if C_{Cr} is assumed to be negligible.

The activities of Fe and Cr in a set of Pt-alloys equilibrated with $FeCr_2O_4$ and Cr_2O_3 were calculated using the ternary Pt-Fe-Cr model and used to compute a value of the free energy of formation of chromite from the elements of -923.5 ± 2.1 kJ/mol (1σ). The value of the free energy of formation of chromite from $Fe + Cr_2O_3 + O_2$ based on the same experiments is -202.7 ± 0.4 kJ/mol (1σ). These values are in excellent agreement with data in the literature, providing a measure of the internal consistency of our ternary alloy model. The activities of chromite in $(Fe,Mg)Cr_2O_4$ are compatible with a one-site symmetric regular solution, yielding an interaction parameter of $+2.14 \pm 0.62$ kJ/mol (1σ) similar within errors to literature evaluations.

Acknowledgments—This work was supported by NASA grant NAG-10423. Discussions with Mike Baker and a written communication with Joe Goldstein led to significant improvements in the quality of this study. Ma Chi is appreciated for his help with the analytical work. The authors thank John Jones and Hugh O'Neill for their constructive reviews. Division contribution #5714.

Associate editor: F. J. Ryerson

REFERENCES

Andersson J.-O. and Sundman B. (1987) Thermodynamic properties of the Cr-Fe system. *CALPHAD* **11,** 83–92.

Arai S. (1987) An estimation of the least depleted spinel peridotite on the basis of olivine-spinel mantle array. *N. Jb. Mineral. Mh.* **1987,** 347–357.

Armstrong J. T. (1988) Quantitative analysis of silicate and oxide materials: Comparison of Monte Carlo, ZAF, and $\phi(\rho Z)$ procedures. In *MicroBeam Analysis* (ed. D. E. Newbury), pp. 239–246. San Francisco Press.

Berger D. and Schwartz K. (1978) Zur Fremddiffusion in Platin. *N. Hutte* **23,** 210–212.

Boericke F. S. and Bangert W. M. (1945) Equilibrium in the reduction of ferrous chromite by hydrogen and energy requirements in the selective reduction of iron in chromite. Reports of Investigation 3813. U.S. Bureau of Mines.

Buddington A. F. and Lindsley D. H. (1964) Iron–titanium oxide minerals and synthetic equivalents. *J. Petrol.* **5,** 310–357.

Carmichael I. S. E. (1967) The iron–titanium oxides of salic volcanic rocks and their associated ferromagnesian silicates. *Contrib. Mineral. Petrol.* **14,** 36–64.

Dick H. J. B. and Bullen T. (1984) Chromian spinel as a petrogenetic indicator in abyssal and alpine-type peridotites and spatially associated lavas. *Contrib. Mineral. Petrol.* **86,** 54–76.

Dunitz J. D. and Orgel L. E. (1957) Electronic properties of transition-metal oxides II. *J. Phys. Chem. Solids* **3,** 318–323.

El Goresy A. (1976) Oxide minerals in lunar rocks. In *Oxide Minerals*, Vol. 3 (ed. D. Rumble), pp. EG1–46. Southern Printing Company.

Evans B. W. and Frost B. R. (1975) Chrome–spinel in progressive metamorphism—A preliminary analysis. *Geochim. Cosmochim. Acta* **39,** 959–972.

Garbers-Craig A. M. and Dippenaar R. J. (1997) Thermodynamic properties of solid Pt-Mn, Pt-Cr, and Pt-Mn-Cr alloys at 1500°C. *Metall. Mater. Trans.* **28B,** 547–552.

Grover J. (1977) Chemical mixing in multicomponent solutions: An introduction to the use of Margules and other thermodynamic excess

functions to represent non-ideal behaviour. In *Thermodynamics in Geology* (ed. D. G. Fraser), pp. 67–97. Reidel.

Haggerty S. E. (1972) Solid solution, subsolidus reduction and compositional characteristics of spinels in some Apollo 15 basalts. *Meteoritics* **7,** 353–370.

Hildebrand J. H. (1929) Solubility. XII. Regular solutions. *J. Am. Chem. Soc.* **51,** 66–80.

Hino M., Higuchi K-I., Nagasaka T., and Ban-ya S. (1994) Phase equilibria and activities of the constituents in FeO · Cr_2O_3-MgO: Cr_2O_3 spinel solid solution saturated with Cr_2O_3. *ISIJ Int.* **34,** 739–745.

Holzheid A. and O'Neill H. St. C. (1995) The Cr-Cr_2O_3 oxygen buffer and the free energy of formation of Cr_2O_3 from high-temperature electrochemical measurements. *Geochim. Cosmochim. Acta* **59,** 475–479.

Jacob K. T. and Alcock C. B. (1975) The oxygen potential of the systems Fe + $FeCr_2O_4$ + Cr_2O_3 and Fe + FeV_2O_4 + V_2O_3 in the temperature range 750–1600°C. *Metall. Trans.* **6B,** 215–221.

Jacob K. T. and Iyengar G. N. K. (1999) Thermodynamics and phase equilibria involving the spinel solid solution $Fe_xMg_{1-x}Cr_2O_4$. *Metall. Mater. Trans.* **30B,** 865–871.

Katsura T. and Muan A. (1964) Experimental study of equilibria in the system FeO-Fe_2O_3-Cr_2O_3 at 1300°C. *Trans. Metall. Soc. AIME.* **230,** 77–84.

Katsura T., Wakihara M., Hara S-I., and Sugihara T. (1975) Some thermodynamic properties in spinel solid solutions with the Fe_3O_4 component. *J. Solid State Chem.* **13,** 107–113.

Kessel R., Beckett J. R., and Stolper E. M. (2001) Thermodynamic properties of the Pt-Fe system. *Am. Mineral.* **86,** 1003–1014.

Klemme S., O'Neill H. St. C., Schnelle W., and Gmelin E. (2000) The heat capacity of $MgCr_2O_4$, $FeCr_2O_4$, and Cr_2O_3 at low temperatures and derived thermodynamic properties. *Am. Mineral* **85,** 1686–1693.

Kofstad P. (1983) *Nonstoichiometry, Diffusion, and Electrical Conductivity in Binary Metal Oxides*. Krieger.

Mason T. O. and Bowen H. K. (1981) Electronic conduction and thermopower of magnetite and iron–aluminate spinels. *J. Am. Ceramic Soc.* **64,** 237–242.

Mattioli G. S., Wood B. J., and Carmichael I. S. E. (1987) Ternary-spinel volumes in the system $MgAl_2O_4$-Fe_3O_4-$\gamma Fe_{3/8}O_4$: Implications for the effect of P on intrinsic f_{O_2} measurements of mantle–xenolith spinels. *Am. Mineral.* **72,** 468–480.

Nafziger R. H. (1973) High-temperature activity–composition relations of equilibrium spinels, olivines, and pyroxenes in the system Mg-Fe-O-SiO_2. *Am. Mineral.* **58,** 457–465.

Nell J. and Wood B. J. (1989) Thermodynamic properties in a multicomponent solid solution involving cation disorder: Fe_3O_4-$MgFe_2O_4$-$FeAl_2O_4$-$MgAl_2O_4$ spinels. *Am. Mineral.* **74,** 1000–1015.

Nell J., Wood B. J., and Mason T. O. (1989) High-temperature cation distributions in Fe_3O_4-$MgAl_2O_4$-$MgFe_2O_4$-$FeAl_2O_4$ spinels from thermopower and conductivity measurements. *Am. Mineral.* **74,** 339–351.

O'Neill H. St. C. and Navrotsky A. (1984) Cation distributions and thermodynamic properties of binary spinel solid solutions. *Am. Mineral* **69,** 733–753.

O'Neill H. St. C. and Dollase W. A. (1994) Crystal structures and cation distributions in simple spinels from powder XRD structural refinements: $MgCr_2O_4$, $ZnCr_2O_4$, Fe_3O_4 and the temperature dependence of the cation distribution in $ZnAl_2O_4$. *J. Phys. Chem. Minerals* **20,** 541–555.

Petric A. and Jacob K. T. (1982) Thermodynamic properties of Fe_3O_4-FeV_2O_4 and Fe_3O_4-$FeCr_2O_4$ spinel solid solutions. *J. Am. Ceramic Soc.* **65,** 117–123.

Pretorius E. B. and Muan A. (1992) Activity–composition relations in platinum–chromium and platinum–vanadium alloys at 1500°C. *J. Am. Ceramic Soc.* **75,** 1361–1363.

Robie R. A., Hemingway B. S., and Fisher J. R. (1978) *Thermodynamic Properties of Minerals and Related Substances at 298.15 K and 1 bar (10^5 Pascals) Pressure and at Higher Temperatures.* Bulletin 1452. U.S. Geological Survey.

Sack R. O. (1982) Spinels as petrogenetic indicators: Activity–composition relations at low pressures. *Contrib. Mineral. Petrol.* **79,** 169–186.

Sack R. O. and Ghiorso M. S. (1991a) Chromian spinels as petrogenetic indicators: Thermodynamics and petrological applications. *Am. Mineral.* **76,** 827–847.

Sack R. O. and Ghiorso M. S. (1991b) An internally consistent model for the thermodynamic properties of Fe–Mg–titanomagnetite–aluminate spinels. *Contrib. Mineral. Petrol.* **106,** 474–505.

Saxena S. K. (1973) *Thermodynamics of Rock-Forming Crystalline Solutions.* Springer-Verlag.

Schwerdtfeger K. and Muan A. (1965) Activity measurements in Pt-Cr and Pd-Cr solid alloys at 1225°C. *Trans. Metall. Soc. AIME.* **233,** 1904–1906.

Shomate C. H. (1944) Ferrous and magnesium chromites: Specific heats at low temperatures. *Ind. Eng. Chem.* **36,** 910–911.

Toker N. Y., Darken L. S., and Muan A. (1991) Phase relations and thermodynamics of the system Fe-Cr-O in the temperature range of 1600°C to 1825°C (1873–2098 K) under strongly reducing conditions. *Metall. Trans.* **22B,** 689–703.

Tretjakov J. D. and Schmalzried H. (1964) Zur Thermodynamik von Spinelphasen (Chromite, Ferrite, Aluminate). *Ber. Bunsenges. Phys. Chem* **69,** 396–402.

Wohl K. (1946) Thermodynamic evaluation of binary and ternary liquid systems. *Trans. Am. Inst. Chem. Eng.* **42,** 215–249.

Wohl K. (1953) Thermodynamic evaluation of binary and ternary liquid systems. *Chem. Eng. Prog.* **49,** 218–219.

Wolfram S. (1999) *The Mathematica Book*. Cambridge University Press.

Woodland A. B. and Wood B. J. (1994) Fe_3O_4 activities in Fe-Ti spinel solid solutions. *Eur. J. Mineral.* **6,** 23–37.